Theoretical study of stereodynamics for the N + H_2/D_2/T_2 reactions*

Li Yong-Qing(李永庆)[a)b)†], Zhao Jin-Feng(赵金峰)[a)], Zhang Yong-Jia(张永嘉)[a)], Chi Xiao-Lin(迟晓琳)[a)], Ding Yong(丁 勇)[a)‡], and Ma Feng-Cai(马凤才)[a)]

[a)] *Department of Physics, Liaoning University, Shenyang* 110036, *China*

[b)] *State Key Laboratory of Molecular Reaction Dynamics, Dalian Institute of Chemical Physics, Chinese Academy of Sciences, Dalian* 116023, *China*

(Received 13 May 2014; revised manuscript received 17 July 2014; published online 10 October 2014)

The effects of isotopic variants on stereodynamic properties for the title reactions have been investigated using a quasi-classical trajectory method based on the first excited state $NH_2(1^2A')$ potential energy surface [Li Y Q and Varandas A J C 2010 *J. Phys. Chem. A* **114** 9644]. The forward–backward symmetry scattering of the differential cross section can be observed, which demonstrates that all these reactions follow the insertion mechanism. Three angle distribution functions $P(\theta_r)$, $P(\phi_r)$, and $P(\theta_r, \phi_r)$ with different collision energies and target molecules H_2/D_2/T_2 are calculated. It is shown that the product rotational angular momentum is not only aligned, but also oriented along the direction perpendicular to the scattering plane. The title reaction is mainly governed by the "in-plane" mechanism through the calculated distribution function $P(\theta_r, \phi_r)$. The observable influences on the rotational polarization of the product by the isotopic substitution of H/D/T can be demonstrated.

Keywords: quasi-classical trajectory method, stereodynamics, potential energy surface, product polarization

PACS: 34.50.Lf, 34.50.–s, 31.15.xv **DOI:** 10.1088/1674-1056/23/12/123401

1. Introduction

In recent decades, the reactivity of atomic nitrogen and its radicals have received considerable attention for their important roles in various fields such as combustion processes and atmospheric chemistry.[1–7] Both experimental and theoretical viewpoints have been adopted to investigate the reaction N + H_2 → NH + H.[8–24] The vibrational and rotational state distributions of the nascent NH molecules were measured using a laser-induced fluorescence technique on the title reaction.[9,11,13] The study of N(^{2}D) + D_2 by using a crossed molecular beam yielded a forward–backward symmetric product angular distribution, which is indicative of insertion dynamics.[25] The early time-resolved spectra provided that the N(^{2}D) + $H_2(X^1\Sigma_g^+)$ → NH $(X^3\Sigma^-)$ + H (^{2}S) reaction products inverted vibrational distributions.[26] The conclusions have been supported by the subsequent theoretical studies based on the London–Eyring–Polanyi–Sato (LEPS) potential energy surface (PES)[27] and first-order configuration interaction (FOCI) PES.[28,29]

A global ground state ($1^2A''$) PES of NH_2 has been presented by Pederson *et al.*[16] The ratios and other aspects of vibration product distributions are in agreement with those from the recent laser-induced fluorescence studies.[9,11] Ho *et al.* reported a ground state PES of the N(^{2}D) + H_2 $(X^1\Sigma_g^+)$ system.[17] The differential cross sections (DCSs) and rate constants of vibrational and rotational distributions have been reported. Owing to the high reactivity of N(^{2}D), Pederson *et al.*[30] reported that a global PES for the second lowest electronic state ($1^2A'$) is dependent on an interpolation technique known as reproducing kernel Hilbert space (RKHS). Also the quasi-classical trajectory (QCT) method was performed on this RKHS PES to investigate the N(^{2}D) + H_2 reaction dynamics.[31] Recently, the new accurate global DMBE-SEC PES for $NH_2(1^2A')$ has been reported by Li and Varandas,[32] which was obtained by fitting *ab initio* energies calculated at a multireferance configuration interaction level with the aug-cc-PVQZ basis set, after relating semiempirically to the dynamical correlation depending on the double many-body expansion-scaled external correlation method.

As mentioned above, most of the previous studies dealt with the experimental and theoretical results containing scalar properties. In fact, in order to gain a comprehensive understanding of this important reaction, the vector properties should also be explored, for they can provide us with a clear view of their direction and the likely polarization of the products. However, to our knowledge, to date few vector properties have been studied for the reaction of N(^{2}D) + H_2 $(X^1\Sigma_g^+)$ → NH $(a^1\Delta)$ + H (^{2}S). In the present work, the quasi-classical trajectory (QCT) method is used to investigate the vector properties of the N (^{2}D) + H_2 $(X^1\Sigma_g^+)$ → NH $(a^1\Delta)$ + H (^{2}S) isotope reactions based on the first excited state $NH_2(1^2A')$ DMBE-SEC PES.

*Project supported by the National Natural Science Foundation of China (Grant Nos. 11474141 and 11274149), the Program of Shenyang Key Laboratory of Optoelectronic Materials and Technology, China (Grant No. F12-254-1-00), the Scientific Research Foundation for Doctors of Liaoning University, the Special Fund Based Research New Technology of Methanol Conversion and Coal Instead of Oil, the China Postdoctoral Science Foundation (Grant No. 2014M550158), and the Program for Liaoning Excellent Talents in University (Grant No. LJQ2014001).

†Corresponding author. E-mail: yqli@lnu.edu.cn

‡Corresponding author. E-mail: yongding@lnu.edu.cn

© 2014 Chinese Physical Society and IOP Publishing Ltd

The rest of this paper is organized as follows. In Section 2, we briefly describe the main details of the theoretical methodologies. The detailed results and discussion of the QCT simulations are presented in Section 3. Finally, the conclusions are drawn from the present studies in Section 4.

2. Theory

2.1. Quasi-classical trajectory calculations

A benchmark QCT procedure is used, which has been carried out in many reaction systems.[33–47] The integration step is set to be 0.1 fs to ensure a convergence of the results. The distance between atom N and the center-of-mass (CM) of the diatomic molecule is set to be 15 Å to ensure no interaction between them. A branch of 0.5×10^5 trajectories is run for each of the reactions N + $H_2/D_2/T_2$. The collision energies are set to be 20 kcal/mol and 50 kcal/mol with the reagent molecules $H_2/D_2/T_2$ ($v=0$ and $j=0$). The orientation of the diatomic molecule and the phase of the diatomic vibrational motion are randomly sampled by a Monte Carlo procedure and the impact parameters are optimized before running the trajectories.

2.2. Vector correlations

The CM reference frame is used in the present investigation. The initial relative velocity vector $\boldsymbol{k}$ of reagent is parallel to the z axis in the CM frame. Scattering plane x–z plane contains $\boldsymbol{k}$ and relative velocity vector $\boldsymbol{k}'$ of the final product. Scattering angle θ_t is the angle between $\boldsymbol{k}$ and $\boldsymbol{k}'$. The ϕ_r and θ_r are the azimuthal and polar angles relating to final rotational angular moment $\boldsymbol{j}'$ respectively.

The distribution function $P(\theta_r)$ describing the $\boldsymbol{k}$–$\boldsymbol{j}'$ correlation can be expanded into a series of Legendre polynomials[48]

$$P(\theta_r)=\frac{1}{2}\sum_k(2k+1)a_0^{(k)}\mathrm{P}_k(\cos\theta_r). \quad (1)$$

The coefficient of the expansion is called the rotational alignment parameter of the product. For $k=2$,

$$a_0^{(2)}=\langle P_2(\cos\theta_r)\rangle=\langle P_2(\boldsymbol{j}\cdot\boldsymbol{k})\rangle=\frac{1}{2}\langle 3\cos^2\theta_r-1\rangle. \quad (2)$$

The dihedral angle distribution function $P(\phi_r)$ describing the $\boldsymbol{k}$–$\boldsymbol{k}'$–$\boldsymbol{j}'$ correlation can be expanded into a Fourier series[48]

$$P(\phi_r)=\frac{1}{2\pi}(1+\sum_{\text{even},n\geq2}a_n\cos n\phi_r+\sum_{\text{even},n\geq1}b_n\sin n\phi_r). \quad (3)$$

The joint probability density function of angles θ_r and ϕ_r can be expressed by

$$P(\theta_r,\phi_r)=\frac{1}{4\pi}\sum_{kq}[k]a_q^kC_{kq}(\theta_r,\phi_r)^*$$
$$=\frac{1}{4\pi}\sum_k\sum_{q\geq0}\left[a_{q\pm}^k\cos q\phi_r-a_{q\mp}^k\sin q\phi_r\right]C_{kq}(\theta_r,0). \quad (4)$$

The full three-dimensional angular distribution associated with $\boldsymbol{k}$–$\boldsymbol{k}'$–$\boldsymbol{j}'$ can be represented by a set of generalized polarization-dependent differential cross sections (PDDCSs) in the CM frame, which is described in Ref. [49].

3. Results and discussion

3.1. Cross section and $\boldsymbol{k}$–$\boldsymbol{k}'$ vector correlation

To show the validity of the QCT method, we calculate the integral cross section in a collision energy range of 1 kcal/mol–20 kcal/mol, which is shown in Fig. 1. The total cross section calculated by Pederson *et al*. based on the RKHS PES is also shown in the figure for comparison.[30] It can be noted that our QCT results based on DMBE-SEC PES are in overall accordance with their results, demonstrating the correctness of QCT calculations. In addition, the calculated threshold energy (about 4.5 kcal/mol) is also in agreement with their result (about 4 kcal/mol).

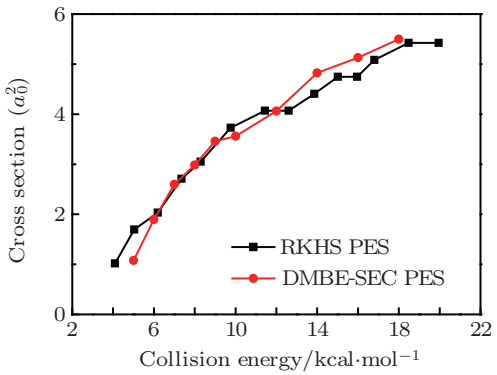


Fig. 1. (color online) Cross section as a function of collision energy for N + H_2 → NH + H calculated by QCT (solid circle line) and similar calculation cited from Ref. [30] (solid square line).

The $\boldsymbol{k}$–$\boldsymbol{k}'$ angle distribution is shown in Fig. 2(a), displaying the calculated DCSs for N + $H_2/D_2/T_2$ ($v=0$, $j=0$) at a collision energy of 20 kcal/mol. Clearly, the NH/ND/NT molecules are mainly scattered forward–backward symmetry. Pederson *et al*.[16] reported a similar forward–backward symmetry scattering in ground state, whereas the results calculated are for the first excited state of NH_2. In fact, it can be comprehended easily due to the resemblant values of barrier and the valley on reaction pathways between both states as can be seen from Fig. 1 in Ref. [50]. In addition, it can be concluded that the dominant angular dependence of the cross section is governed by the insertion mechanism. With the enhancement of target molecule mass, the backward scattering lowers and forward scattering increases slightly. From Fig. 2(b) we can see that the forward–backward symmetry scattering also exists when the collision energy is 50 kcal/mol. Particularly, the forward scattering becomes more obvious when considering

the isotope effects, i.e., the larger the target molecular mass, the higher the forward scattering frequency will be. That is to say, with the enhancement of collision energy, the scattering of isotope effect becomes more pronounced. In addition, it should be noted that the trends of N + H_2 reaction between 50°–90° are different from the other isotope reaction trends as indicated by comparing Fig. 2(b) with Fig. 2(a), which could explain the fact that larger collision energy could have larger influence on DCSs.

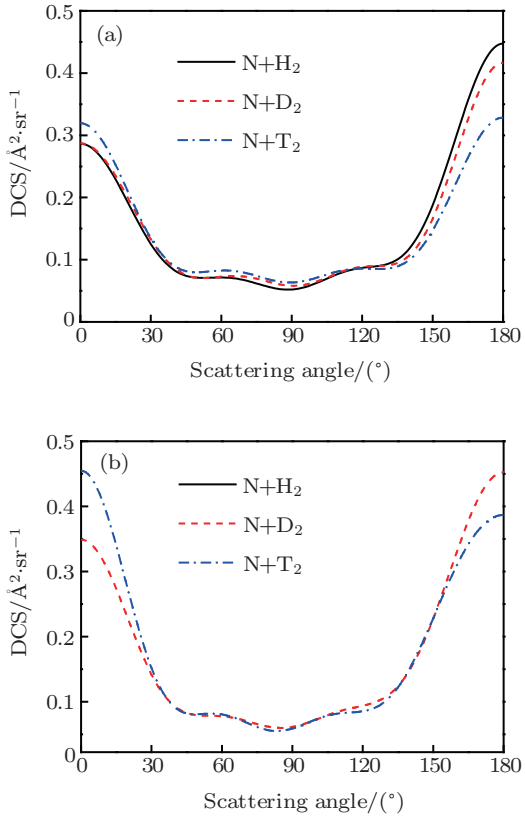


Fig. 2. (color online) Variations of differential cross sections for the reactions N + H_2/D_2/T_2 proceeding on the DMBE-SEC PES with scattering angle at the collision energies of (a) 20 kcal/mol and (b) 50 kcal/mol.

3.2. k–j' vector correlation

The relative alignment of the k, j' vectors and the relative orientation of the k, k', and j' vectors could be described by $P(\theta_r)$ and $P(\phi_r)$ distributions, respectively, which can provide an overall representation of the polarization of rotational angular momentum vector of NH molecular in the scattering plane. Figure 3 shows the distributions of $P(\theta_r)$ for the reactions N + H_2/D_2/T_2 at collision energies of 20 kcal/mol and 50 kcal/mol. The distributions of $P(\theta_r)$ are maximal for θ_r at 90° and symmetric with respect to 90°. The j' is distributed with cylindrical symmetry in the scattering frame of the product, and the direction of j' is perpendicular to k direction. However, as shown in Fig. 3, if the mass of the molecule target isotope transfers, the changes of the peaks of $P(\theta_r)$ distribution are smaller, which indicates that the mass effect of molecule target isotopic variant becomes inconspicuous. It may be explained that the mass of attacking atom (N) is too large relative to the targets (H_2/D_2/T_2) to exert a large influence on the product rotational alignment. In Fig. 3(b), the peaks of the three reactions are almost the same, indicating that large collision energy almost has no effect on the rotational alignment. The values in Table 1 could be further used to demonstrate that the increase of the target molecule mass leads to little change in the $P(\theta_r)$ distribution. In addition, it is worth mentioning that with the enhancement of target molecule mass, the values of $P(\theta_r)$ distribution at $\theta_r = 0°$ and 180° become lower gradually. It could be demonstrated that with the increase of the target molecule mass, the polarization parallel to the direction of the relative velocity of reactants becomes weaker.

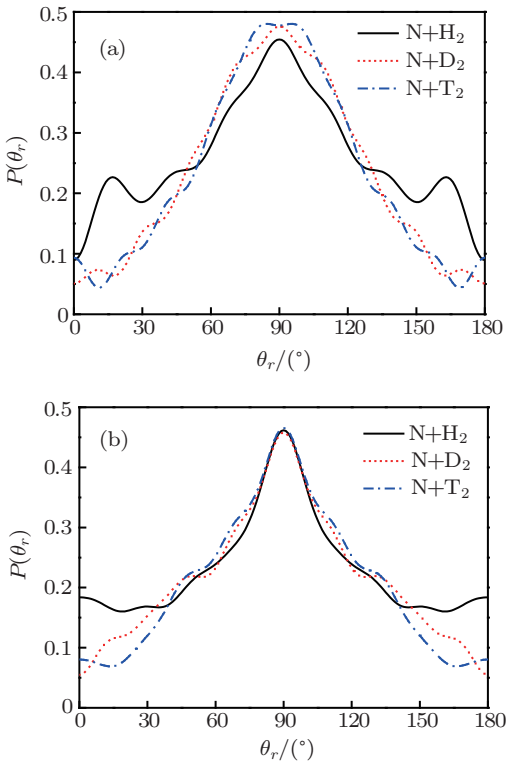


Fig. 3. (color online) Rotational polarizations of the NH/ND/NT products from the reactions N + H_2/D_2/T_2, and distributions of $P(\theta_r)$ reflecting the k–j' vector correlation at the collision energies of (a) 20 kcal/mol and (b) 50 kcal/mol.

Table 1. Product rotational alignment parameters $\langle P_2(j' \cdot k)\rangle$ calculated on the DMBE-SEC PES at collision energies of 20 kcal/mol and 50 kcal/mol for the reactions N+H_2/D_2/T_2.

Collision energy	N + H_2 →NH + H	N + D_2 →ND + D	N + T_2 →NT + T
20 kcal/mol	–0.3908	–0.4059	–0.4094
50 kcal/mol	–0.4097	–0.4111	–0.4297

3.3. k–k'–j' vector correlation

The profiles of dihedral angle distribution $P(\phi_r)$ describing the k–k'–j' vector correlations at two collision energies of 20 kcal/mol and 50 kcal/mol are shown in Fig. 4. It can be seen

that in contrast to the symmetric feature of the $P(\theta_r)$ distribution, $P(\phi_r)$ distributions tend to be asymmetric obviously with respect to the $\boldsymbol{k}$–$\boldsymbol{k}'$ scattering plane (or about $\phi_r = 180°$). The peaks appearing at 90° and 270° imply that the products tend to align along the y axis (perpendicular to the scattering plane). We can infer roughly that the reaction is much easier to happen when the reactant relative velocity is parallel to the plane containing three atoms, or the PES tends to rotate the three atoms into a plane parallel to $\boldsymbol{k}$ to proceed with the reaction. That is to say, the products have a preference for a counterclockwise rotation in the plane parallel to the scattering plane, the reaction is mainly governed by "in-plane" mechanism. The peaks at 270° are much lower than those at 90°, which means that $\boldsymbol{j}'$ tends to be oriented along the positive direction of the y axis. i.e., the strong polarization of product rotational angular momentum occurs. At the lower collision energy of 20 kcal/mol, the peaks at $\phi_r = 90°$ become lower whereas the peaks at 270° become higher with the enhancement of the target molecule mass. At the higher collision energy of 50 kcal/mol, in contrast, the distribution of $P(\phi_r)$ shows that the peaks at $\phi_r = 90°$ and 270° become higher with the enhancement of the target molecule mass.

In order to show the angular momentum polarization clearly, the distributions of $P(\theta_r, \phi_r)$ are calculated (Fig. 5), which represent the average scattering angles of the full distribution $P(\omega_t, \omega_r)$. The tomographical features of the distributions of the $P(\theta_r, \phi_r)$ peaks at $(\pi/2, 3\pi/2)$ are in good accordance with those of the distributions of $P(\theta_r)$ and $P(\phi_r)$. The plot of the distribution of $P(\theta_r, \phi_r)$ indicates that the products are preferentially polarized in the direction perpendicular to the scattering plane and the reactions are mainly dominated by "in-plane" mechanisms.

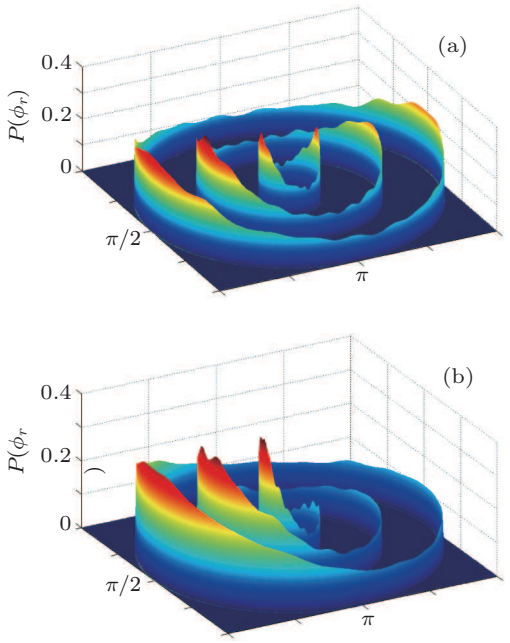


Fig. 4. (color online) Rotational polarization of the NH/ND/NT products from the reactions N + H_2/D_2/T_2 (from outer to inner), and distributions of $P(\phi_r)$ reflecting the $\boldsymbol{k}$–$\boldsymbol{k}'$–$\boldsymbol{j}'$ vector correlation at the collision energies of (a) 20 kcal/mol and (b) 50 kcal/mol.

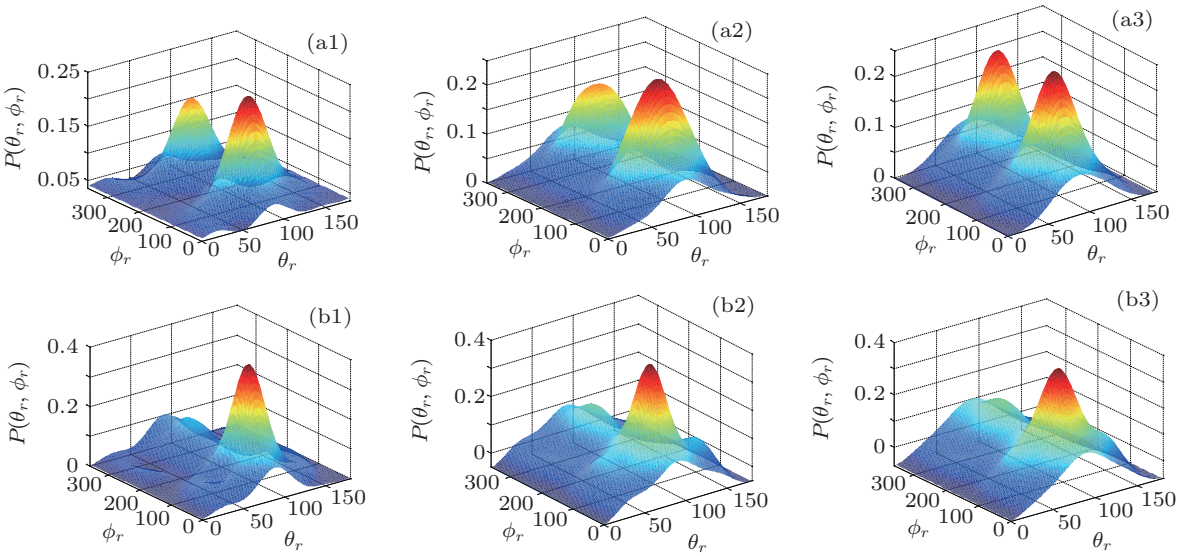


Fig. 5. (color online) Polar plots of $P(\theta_r, \phi_r)$ distribution averaged over all scattering angles for the reactions N + H_2/D_2/T_2 (from 1 to 3) at the collision energies of (a) 20 kcal/mol and (b) 50 kcal/mol.

4. Conclusions

In this work, the stereodynamics of N + H_2/D_2/T_2 → NH/D/T + H/D/T isotope reactions is studied using QCT method based on the first excited state $NH_2(1^2A')$ DMBE-SEC PES. The 0.5×10^5 trajectories run in each initial condition to investigate the effects on the product alignment and

the orientation. The forward–backward scatterings at collision energies of 20 kcal/mol and 50 kcal/mol are investigated, and the insertion mechanism could be concluded through calculating the DCSs. The three angle distributions $P(\theta_r)$, $P(\phi_r)$, and $P(\theta_r, \phi_r)$ are also calculated. The results show that the product rotational angular momentum j' is not only aligned, but also oriented along the direction perpendicular to the scattering plane. The calculated distribution of $P(\theta_r, \phi_r)$ indicates that the NH/ND/NT products are preferentially polarized in the direction perpendicular to the scattering plane and the reactions are mainly dominated by "in-plane" mechanism.

References

[1] Bozzelli J W and Dean A M 1995 *Int. J. Chem. Kinet.* **27** 1097
[2] Tomeczek J and Gradon B 2003 *Combust. Flame* **133** 311
[3] Woodall J, Agundez M, Markwick-Kemper A J and Millar T J 2007 *Astron. Astrophys.* **466** 1197
[4] Hellman A, Baerends E J, Biczysko M, Bligaard T, Christensen C H, Clary D C, Dahl S, Van Harrevelt R, Honkala K, Jonsson H, Kroes G J, Luppi M, Manthe U, Norskov J K, Olsen R A, Rossmeisl J, Skulason E, Tautermann C S, Varandas A J C and Vincent J K 2006 *J. Phys. Chem. B* **110** 17719
[5] Miller J A and Bowman C T 1989 *Prog. Energy Combust. Sci.* **15** 287
[6] Hughes K J, Tomlin A S, Hampartsoumian E, Nimmo W, Zsely I G, Ujvari M and Turanyi T 2001 *Combust. Flame* **124** 573
[7] Hayhurst A N and Hutchinson E M 1998 *Combust. Flame* **114** 274
[8] Balucani N, Alagia M, Cartechini L, Casavecchia P, Volpi G G, Pederson L A and Schatz G C 2001 *J. Phys. Chem. A* **105** 2414
[9] Umemoto H and Matsumoto K 1996 *J. Chem. Phys.* **104** 9640
[10] Balucani N, Casavecchia P, Banares L, Aoiz F J, Gonzalez-Lezana T, Honvault P and Launay J M 2006 *J. Phys. Chem. A* **110** 817
[11] Umemoto H, Asai T and Kimura Y 1997 *J. Chem. Phys.* **106** 4985
[12] Balucani N, Cartechini L, Capozza G, Segoloni E, Casavecchia P, Volpi G G, Aoiz F J, Banares L, Honvault P and Launay J M 2002 *Phys. Rev. Lett.* **89** 013201
[13] Umemoto H, Terada N and Tanaka K 2000 *J. Chem. Phys.* **112** 5762
[14] Rao B J and Mahapatra S 2007 *J. Chem. Phys.* **127** 244307
[15] Honvault P and Launay J M 1999 *J. Chem. Phys.* **111** 6665
[16] Pederson L A, Schatz G C, Ho T S, Hollebeek T, Rabitz H, Harding L B and Lendvay G 1999 *J. Chem. Phys.* **110** 9091
[17] Ho T S, Rabitz H, Aoiz F J, Banares L, Vázquez S A and Harding L B 2003 *J. Chem. Phys.* **119** 3063
[18] Lin S Y, Banares L and Guo H 2007 *J. Phys. Chem. A* **111** 2376
[19] Defazio P and Petrongolo C 2006 *J. Chem. Phys.* **125** 064308
[20] Defazio P and Petrongolo C 2007 *J. Chem. Phys.* **127** 204311
[21] Chu T S, Han K L and Varandas A J C 2006 *J. Phys. Chem. A* **110** 1666
[22] Lin S Y and Guo H 2006 *J. Chem. Phys.* **124** 031101
[23] Castillo J F, Bulut N, Banares L and Gogtas F 2007 *Chem. Phys.* **332** 119
[24] Chu T S, Duan Y B, Yuan S P and Varandas A J C 2007 *Chem. Phys. Lett.* **444** 351
[25] Alagia M, Balucant N, Cartechini L, Casavecchia P, Volpi G G, Pederson L A and Schatz G C 1999 *J. Chem. Phys.* **110** 8857
[26] Dodd J A, Lipson S J, Flanagan D J, Blumberg W A M, Person J C and Green B D 1991 *J. Chem. Phys.* **94** 4301
[27] Suzuki T, Shihia Y, Sato T, Umemoto H and Tsunashima S 1993 *J. Chem. Soc., Faraday Trans.* **89** 995
[28] Kobayashi H, Takayangagi T and Tsunashima S 1997 *Chem. Phys. Lett.* **277** 20
[29] Kobayashi H, Takayangagi T, Yokoyama K, Sato T and Tsunashima S 1995 *J. Chem. Soc., Faraday Trans.* **91** 3771
[30] Pederson L A, Schatz G C, Ho T, Hollebeek T, Rabitz H and Harding L B 2000 *J. Phys. Chem. A* **104** 2301
[31] Akpinar S, Defazio P, Gamallo P and Petrongolo C 2008 *J. Chem. Phys.* **129** 174307
[32] Li Y Q and Varandas A J C 2010 *J. Phys. Chem. A* **114** 9644
[33] Liu L S and Shi Y 2011 *Chin. Phys. B* **20** 013404
[34] Yao C X and Zhao G J 2013 *Chin. Phys. B* **22** 083403
[35] Ma J J, Zou Y and Liu H T 2013 *Chin. Phys. B* **22** 063402
[36] Zhao D, Chu T S and Hao C 2013 *Chin. Phys. B* **22** 063401
[37] Yu Y J and Xiu Q 2011 *Chin. Phys. B* **20** 123402
[38] Han K L, He G Z and Lou N Q 1996 *J. Chem. Phys.* **105** 8699
[39] Wei Q 2014 *Chin. Phys. B* **23** 023401
[40] Yue X F 2013 *Chin. Phys. B* **22** 113401
[41] Sha G Y, Yuan J C and Meng C G 2014 *Chin. Phys. B* **23** 018202
[42] Han K L, Zhang L, Xu D L, He G Z and Lou N Q 2001 *J. Phys. Chem. A* **105** 2956
[43] Wang Y P, Zhao M Y and Yao S H 2013 *Chin. Phys. B* **22** 128201
[44] Tong H, Yang Y B and Shi Z Y 2013 *Acta Phys. Sin.* **62** 132101 (in Chinese)
[45] Wei L, Zhou H W and Zhang L 2013 *Chin. Phys. B* **22** 096201
[46] Wang M L, Han K L and He G Z 1998 *J. Phys. Chem. A* **102** 10204
[47] Chen M D, Han K L and Lou N Q 2003 *J. Phys. Chem.* **118** 4463
[48] Aoiz F J, Brouard M and Enriquez P A 1996 *J. Chem. Phys.* **105** 4964
[49] Orr-Ewing A J and Zare R N 1994 *Ann. Rev. Phys. Chem.* **45** 315
[50] Li Y Q and Varandas A J C 2012 *Int. J. Quantum Chem.* **112** 2932